Comparison of the Four Anhydrous Polymorphs of Carbamazepine and the Crystal Structure of Form I

ADAM L. GRZESIAK, MEIDONG LANG, KIBUM KIM, ADAM J. MATZGER

Department of Chemistry and the Macromolecular Science and Engineering Program, The University of Michigan, Ann Arbor, Michigan 48109-1055

Received 18 November 2002; revised 31 March 2003; accepted 2 April 2003

ABSTRACT: For decades, carbamazepine (CBZ) has served as a model compound for groups engaged in the study of crystal polymorphism. Despite considerable effort, crystal structures for only three of its four anhydrous forms have previously been determined. Herein, we report the first single crystal X-ray structure of the high temperature modification of CBZ (form I). Form I crystallizes in a triclinic cell (P-1) having four inequivalent molecules with the following lattice parameters: $a = 5.1705(6)$, $b = 20.574(2)$, $c = 22.245(2)$ Å, $\alpha = 84.12(4)$, $\beta = 88.01(4)$, and $\gamma = 85.19(4)^\circ$. Furthermore, we compare the physical properties of the four anhydrous polymorphs of CBZ, including the first comprehensive characterization of form IV. Substantial differences are seen among these forms by powder X-ray diffraction, infrared spectroscopy, thermomicroscopy, and differential scanning calorimetry. These data are correlated to their respective crystal structures for the first time. We have found that all polymorphs possess identical strong hydrogen bonding patterns, similar molecular conformations, and stabilities that are within 0.7 kcal/mol of each other. © 2003 Wiley-Liss, Inc. and the American Pharmacists Association J Pharm Sci 92:2260–2271, 2003

Keywords: polymorphism; crystal structure; X-ray diffractometry; calorimetry (DSC); hydrogen bond

INTRODUCTION

The role of crystal packing in determining many of the important properties of solid materials has led to increased recognition of the phenomenon of crystal polymorphism.[1–5] For example, the ability of a pharmaceutical to exist as more than one crystalline polymorph, supramolecular isomers that differ only in molecular packing,[4] creates a situation in which one crystal form may have a favorable dissolution rate, equilibrium solubility, and absorption whereas another is an ineffective therapeutic agent.[6] Although the incidence of polymorphism in the Cambridge Structural Database (CSD) is not high,[a] with only 3% of organic compounds displaying more than one molecular packing arrangement,[3,7] the phenomenon is quite common in pharmaceutical solids where nearly one-third have true polymorphs.[8] This discrepancy can be explained by the link between effort expended and the number of polymorphs discovered, with more widely studied pharmaceuticals revealing considerably more forms.[9] Investigators have sought to understand the factors contri-

Supplementary material: X-ray crystallographic information file (CIF) of triclinic CBZ (form I) is available.

Correspondence to: Adam J. Matzger (Telephone: 734-615-6627; FAX: 734-615-8553; E-mail: matzger@umich.edu)

Journal of Pharmaceutical Sciences, Vol. 92, 2260–2271 (2003)
© 2003 Wiley-Liss, Inc. and the American Pharmacists Association

[a]Because the CSD only contains phases deemed of sufficient interest to determine the structure, there is an inherent bias against the presence of polymorphs. The statistics for pharmaceuticals are probably more representative because each polymorph would be considered worthy of structural determination although each may not necessarily be amenable to analysis by single crystal X-ray diffraction.

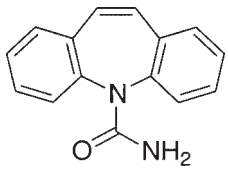

carbamazepine

Structure 1. Structure of CBZ.

buting to polymorphism including hydrogen bonding, molecular size, and conformational flexibility.[10–12] However, the question of how many polymorphs a particular compound will give rise to cannot be estimated at present.

Carbamazepine (CBZ) (Structure 1), an anticonvulsant used to treat epilepsy and trigeminal neuralgia, has served as a model compound for many groups studying crystal polymorphism.[13–32] This important anticonvulsant has been found to crystallize as four different anhydrous polymorphs,[13–32] three of which have been structurally characterized by single crystal X-ray diffraction. The first was found to crystallize in a primitive monoclinic cell (form III).[15,16,23] This was followed by the structure of the trigonal modification (form II)[22] and recently a *C*-centered monoclinic polymorph (form IV).[32]

A longstanding question in CBZ polymorphism has been the identification of the high temperature modification (form I). Although the structure could not be determined, recent work[28] on this phase found a triclinic cell with a volume of 2389 Å^3. This implies that there are either four or eight independent molecules in the unit cell, depending on the space group assignment ($Z' = 4$ for P-1 or $Z' = 8$ for $P1$). This would make the triclinic structure substantially more complex than the other three forms, each of which contains one molecule in the asymmetric unit. Furthermore, a statistical analysis of the CSD (October 2001 version) finds the incidence of structures with $Z' = 4$ in P-1 is 0.37% (188 of 50835 structures) and that there are only nine reported examples of $Z' = 8$ of the 2233 structures in $P1$ (0.40%).[b] Considering the rarity of cells with four or eight asymmetric molecules in the unit cell, further studies of form I were necessary. Furthermore, to study the relationship between the recently prepared form IV and the other CBZ polymorphs, the molecular packing of the triclinic form was of intense interest.

Herein, we report the single crystal X-ray structure of form I (triclinic) of CBZ and compare the physical properties of the four anhydrous polymorphs of this compound, including the first comprehensive characterization of form IV. A structural comparison reveals that the conformation and sense of dimerization remains unchanged among these four modifications, a unique attribute for a highly polymorphic compound.[33–36]

There has been much confusion about the naming of CBZ polymorphs (Table 1). In particular, the morphologically similar trigonal and triclinic forms are difficult to distinguish from one another without the aid of powder X-ray diffraction (PXRD) and/or careful differential scanning calorimetry (DSC) analysis. To definitively identify each of the four anhydrous polymorphs of CBZ, we have reexamined the reported data for the anhydrous polymorphs of CBZ in the literature.[13–32] These were compared with our own set of PXRD, DSC, and infrared (IR) spectroscopy data that are, for the first time, correlated to the crystal structures of each form.

EXPERIMENTAL

Materials

Commercial CBZ (99%, powder) was obtained from Sigma (St. Louis, MO), and stored at 5°C. Ethanol (USP grade, absolute) was bought from Pharmco Products Inc. (Brookfield, CT). Methanol (ACS grade) was purchased from Fisher Scientific (Pittsburgh, PA). All solvents were used directly. Hydroxypropyl cellulose (powder, M_w 60,000) was obtained from Scientific Polymer Products, Inc. (Ontario, NY) and used directly.

Preparation of CBZ Polymorphs

Triclinic CBZ (form I) suitable for single crystal X-ray diffraction was prepared from the melt in a vacuum-sealed capillary. The capillary was then heated to 192.0°C to ensure complete melting of the compound and the temperature decreased to 183.5°C at a rate of 8.0°C/min. At this temperature, nucleation occurred within minutes forming triclinic crystals suitable for analysis by single crystal X-ray diffraction. Bulk form I was obtained by heating 0.3 g of commercial CBZ or recrystallized P-monoclinic at 150°C for 3 h.

[b]The difficulty associated with determination of structures with more than one molecule in the asymmetric unit will lower their frequency in the CSD below their natural occurrence rate.

Table 1. Nomenclature of the Four CBZ Polymorphs[a]

Year	Reference	Triclinic	Trigonal	*P*-Monoclinic	*C*-Monoclinic	Method of Confirmation
1968	13	I	—	III	—	Melting behavior
1975	14	C_3	C_2	C_1	—	PXRD, IR
1981	15,16	—	—	Monoclinic	—	Crystal structure
1984	17	III	II	I	—	PXRD, DSC
1984	18	III	II	I	—	PXRD, DSC
1986	19	I	II, IV	III	—	PXRD, DSC
1986	20	α	—	β	—	PXRD, DSC
1987	21	I	—	III	II[b]	PXRD, DSC
1987	22	—	α, Trigonal	β	—	Trigonal structure, PXRD, DSC, IR
1991	24	I	—	III	—	DSC, preparation
1991	25	γ	α	β	—	Preparation
1992	26	I	—	III	—	IR, melting behavior
1996	27	I	—	III	—	PXRD
1997	28	Triclinic	—	—	—	Cell data, PXRD
2000	29	—	α	β	—	PXRD, SEM
2000	30	I	—	III	—	PXRD, DSC
2000	31	I	—	III	II[b]	PXRD, DSC, IR
2002	32	—	—	—	IV, *C*-Monoclinic	Crystal structure
	This study	I	II	III	IV	XRD, DSC, IR

[a]Each form was verified by the listed method as well as the method of preparation of each form.
[b]These forms are most similar to *C*-monoclinic CBZ, however, differences noted in the text exist.

Trigonal CBZ (form II) was prepared by dissolving 0.96 g of commercial CBZ in 20 mL of ethanol at 80°C. The solution was slowly cooled to room temperature and then cooled further to 5°C for 5 h. The needles were collected by filtration and dried under reduced pressure. *P*-monoclinic CBZ (form III) was crystallized by slow evaporation of an ethanol solution (16.5 mg/mL) at room temperature. *C*-monoclinic CBZ (form IV) crystallization was performed by slow evaporation of methanol solutions (16.5 mg/mL) at room temperature in the presence of hydroxypropyl cellulose.[32,37] Seeding of supersaturated methanol solutions (155 mg/mL) at room temperature also produced form IV. Crystals were harvested 10 h after the seed crystal was added.

Single Crystal X-ray Diffraction

Single crystal X-ray diffraction data of the triclinic form of CBZ was recorded on a Bruker SMART CCD-based X-ray diffractometer equipped with an LT-2 low temperature device and MoKα source (λ = 0.71073 Å). The structure was solved and refined using the Bruker SHELXTL (version 5.10) software package. All non-hydrogen atoms were refined anisotropically with the hydrogen atoms located on a difference Fourier map and allowed to refine independently.

PXRD

PXRD data were recorded at room temperature on a Bruker AXS D_8 Advance powder diffractometer at 40 kV, 40 mA with a CuKα source (λ = 1.5406 Å) between 3 and 90° 2θ with a scan speed of 0.2 s/step and a step size of 0.038°. Samples, ground into powders with an agate mortar and pestle, were measured on a low background quartz plate in an aluminum holder.

Fourier Transform Infrared Spectroscopy (FTIR)

FTIR spectra were recorded on a Perkin-Elmer Spectrum BX FTIR system, equipped with a deuterium triglycine sulfate detector. The scan range was 600–4000 cm^{-1}, using eight scans per spectrum with a resolution of 1 cm^{-1}. Spectra were obtained in the transmission mode in KBr pellets. Spectra were also taken of pure crystalline samples using IR microscopy to compare the effects of grinding and pressure on the samples. A Perkin-Elmer Spectrum GX FTIR system,

equipped with an Auto IMAGE system camera and microscope, was used to collect the IR microscopy spectra.

Thermomicroscopy

Thermomicroscopy was performed with a Mettler Toledo FP82HT hot stage connected to an FP 90 control processor and viewed under polarized light with a Leica DMLP microscope. Samples of each of the four polymorphs were heated from 50 to 200°C at a rate of 10°C/min for initial observation. Upon viewing thermal transformations in forms II, III, and IV, each of these was converted completely and the samples were then removed from the hot stage and identified using PXRD.

DSC

Thermograms of the samples were recorded on a Perkin-Elmer DSC 7 connected to a Perkin-Elmer TAC 7/DX thermal analysis controller with Pyris software (version 3.81). Samples (2–3 mg weighed to a precision of 0.005 mg) were placed in aluminum pans and the lids were crimped using a Perkin-Elmer crimper. Thermal behavior of the samples was studied under a nitrogen purge at various heating rates, covering a temperature range of 30–210°C. The instrument was calibrated with an indium standard.

RESULTS AND DISCUSSION

Single Crystal X-ray Diffraction

Single crystal X-ray analysis of form I at 158(2) K revealed a triclinic lattice: $a = 5.1705(6)$, $b = 20.574(2)$, $c = 22.245(2)$ Å, $\alpha = 84.12(4)$, $\beta = 88.01(4)$, and $\gamma = 85.19(4)°$. This confirmed the lattice parameters previously determined,[28] with the expected volume contraction from low temperature collection.[c] The asymmetric unit consists of four molecules (Fig. 1) that each form hydrogen-bonded *anti* dimers through the carboxamide donor and carbonyl acceptor as in the other three modifications of the drug. Graph set analysis[38,39] revealed that these are R2,2(8) dimers. However,

[c]X-ray structural analysis: Crystal size 0.04 × 0.04 × 0.60 mm, triclinic, *P*-1 (no. 2), $a = 5.1705(6)$, $b = 20.574(2)$, $c = 22.245(2)$ Å, $\alpha = 84.12(4)$, $\beta = 88.01(4)$, $\gamma = 85.19(4)$, $V = 2344.8(5)$ Å^3, $Z = 8$, $T = 158(2)$ K, calculated density = 1.339 g/cm^3, $\mu = 0.086$ mm^{-1}, (MoKα) = 0.71073 Å, scan range 4.00 2θ 46.74, 6768 unique reflections, 842 parameters, goodness of fit on $F^2 = 0.996$, and for I > 2(I) $R = 0.0506$, $R_w = 0.0893$.

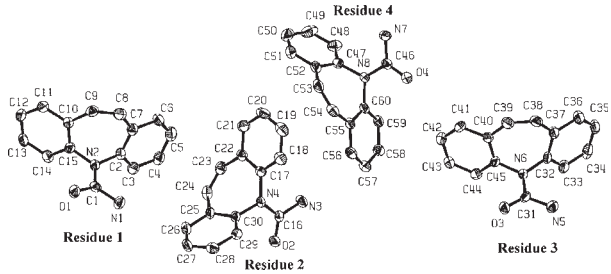

Figure 1. Thermal ellipsoid plot of triclinic CBZ showing the four inequivalent molecules in the unit cell.

only two dimers are centrosymmetric, formed between identical residues (Fig. 2), whereas the other unique dimer is pseudocentrosymmetric and consists of inequivalent 1,3 residue pairs, where the two N–H···O hydrogen bonds differ by <0.1 Å.

For comparative conformational analysis, each of the four inequivalent molecules of form I and also those of the other three forms were computationally overlaid using the OFIT function of XP Interactive Molecular Graphics (version 5.10, Bruker AXS). The largest root mean square deviation between atomic positions among these four forms was <0.15 Å, as observed in the overlay fits of individual molecules. Furthermore, because all forms exist as dimers in the solid state, all inequivalent R2,2(8) dimer pairs of the four forms were overlaid and displayed <0.40 Å root mean square deviation, demonstrating a consistent sense of conformation and dimerization throughout the four forms with regard to their strong hydrogen bonding network. This stands in contrast to conformational polymorphism or changes in strong hydrogen bonding networks which are observed in other tetramorphic or higher order polymorphic systems: sulfapyridine, pyrazinecarboxamide, sulfathiazole, and 5-methyl-2-[(2-nitrophenyl)amino]-3-thiophenecarbonitrile.[33–36] Thus, CBZ is an excellent example of crystal polymorphism in which conformation and strong hydrogen-bonding scheme remains constant throughout all of its forms.

The differences among crystal forms lie solely in the packing of the carboxamide dimer units. This can be described by the pattern of weak C–H···O interactions (<2.60 Å from the normalized, 1.083 Å for C–H, position of the hydrogen), which are prevalent throughout all of the four forms (Fig. 2), using graph sets.[38,39] Both monoclinic forms have similar, yet distinct interactions and the trigonal and triclinic forms are also structurally related. The monoclinic forms both have infinite C(7)

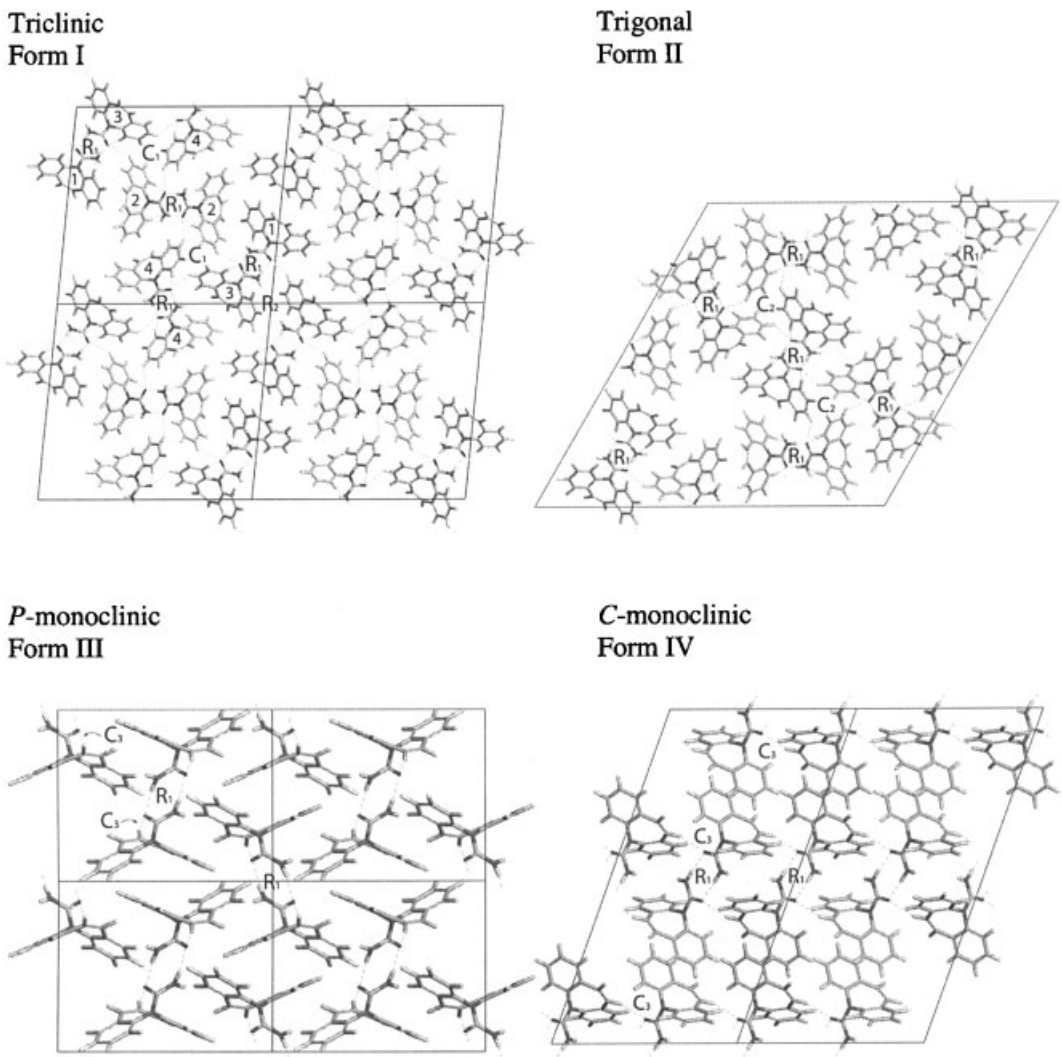

Figure 2. Packing diagrams of all four forms of CBZ showing hydrogen-bonding patterns. The notation indicates the position of important hydrogen-bonding patterns and is as follows: $R_1 = R2,2(8)$; $R_2 = R2,4(20)$; $C_1 = C3,6(24)$; $C_2 = C1,2(8)$; $C_3 = C(7)$. The Arabic numerals on form I correspond to the respective residues.

chains through a vinylic hydrogen of the azepine ring and an oxygen acceptor. The C–H···O bonds that link the dimer units of both monoclinic forms have lengths of 2.48 and 2.28 Å for forms III and IV, respectively. The two polymorphs with needle morphologies, triclinic and trigonal, are strikingly similar in their weak hydrogen bond patterns. In both structures, each oxygen acts as an acceptor to hydrogens from two nearby carbons. The position of the carbon donors is identical in both forms: one is *ortho* to the urea from an identical residue in an adjacent unit cell and the other is *para* to the urea from the nearest donor residue. Perhaps because of the high symmetry of the trigonal system, there is only one significant pattern of weak hydrogen bonding. This is a C1,2(6) chain that spirals about the needle axis of the crystal.[d] These spirals are all linked to each other through the R2,2(8) dimer units, thus creating an infinite network. The triclinic form has similar spiral chains about its needle axis. However, because the spirals involve three inequivalent molecules (residues 2, 3, and 4) they are termed C3,6(24) chains. Also present in the triclinic structure are R2,4(20) rings involving residues 1 and 3. These rings along with the R2,2(8) dimer rings link the spiral chains causing

[d]The needle axes of both triclinic and trigonal were determined using BFDH morphology prediction as implemented in Cerius[2], version 4.2.

an extended three-dimensional network similar to that of the trigonal form.

Nomenclature of CBZ Polymorphs

From Table 1 it is obvious that there is inconsistency in the naming of CBZ polymorphs, leading to confusion and the misidentification of forms. The conclusions presented here are based on careful comparison of simulated PXRD patterns to our experimental diffraction data. These are then correlated to DSC thermograms, IR spectra, and methods of preparation of each form and compared with the data of the previous investigators.

We note that there was a previous attempt to clarify the CBZ nomenclature in which the authors identified one of their forms as being trigonal based on literature references.[24] However, it is actually the triclinic form they present. This form was produced by heating *P*-monoclinic, which is well known to produce triclinic CBZ.[14,17–19,21,26–28,30,31] However, this occurred several years before the elucidation of the triclinic lattice.[28] Because the trigonal and triclinic forms are morphologically similar, without extreme care in analyzing PXRD patterns and precise DSC measurements,[17–19] differentiating these forms is not a trivial task.

There have been two previous reports of the existence of four CBZ polymorphs.[13,19] One indicates the presence of four forms of CBZ based on thermomicroscopy.[13] These forms are identified by their melting points, with the highest melting modification termed form I and the next highest as form II, etc. Because melting points are dependent on heating rates it is difficult to conclude which forms were being observed. Furthermore, other characterization methods are not offered and thus comparisons with other preparations cannot be made. More extensive data are provided in another report of four anhydrous polymorphs of CBZ.[19] However, forms II and IV are deemed the same based on peak positions and intensities of the PXRD diffractograms. There are three peaks lacking in the form II PXRD pattern, which are likely a product of preferred orientation of the trigonal form because they are present in simulated and our experimental PXRD patterns. Furthermore, it has been previously suggested that a mixture of modifications[21] would account for differences these authors observed in the IR spectra. Thus, only three anhydrous polymorphs were identified rather than the four reported. By contrast, a polymorph prepared by dehydration,[21,31] designated by the authors as form II, has several characteristics of *C*-monoclinic prepared in our lab. The published PXRD, DSC, and IR data for the dehydrated form most closely resembles *C*-monoclinic CBZ. However, discrepancies in the carbonyl stretching frequency in the IR spectrum[21] and the appearance of an amorphous impurity in the DSC[31] indicates the material described is not in pure form and no structural data is offered.

PXRD

The most reliable way to distinguish the four polymorphs of CBZ is with PXRD (Fig. 3). Form I has diagnostic peaks at $2\theta = 7.92$, 9.37, 12.28, and 19.99. Form II is recognizable because it has few high intensity peaks at $2\theta = 8.68$, 13.26, 18.56, and 24.54. The indicative peaks for form III occur at $2\theta = 15.36$, 19.56, 25.00, and 27.47. Form IV has characteristic peaks at $2\theta = 14.11$, 17.89, 21.79, and 33.11. A complete list of all peaks and their relative intensities are presented in Table 2. These values compare well with simulated PXRD patterns in terms of 2θ positions with the expected small shifts resulting from the different temperatures of data collection. However, the intensities vary, especially for forms I and II, because of preferred orientation of samples in the powder X-ray experiment.

FTIR Spectroscopy

The three main regions for identifying and distinguishing the polymorphs of CBZ are 3500–3392, 1731–1629, and 1427–1317 cm^{-1} (Fig. 4, Table 3). IR microscopy of single crystals of each

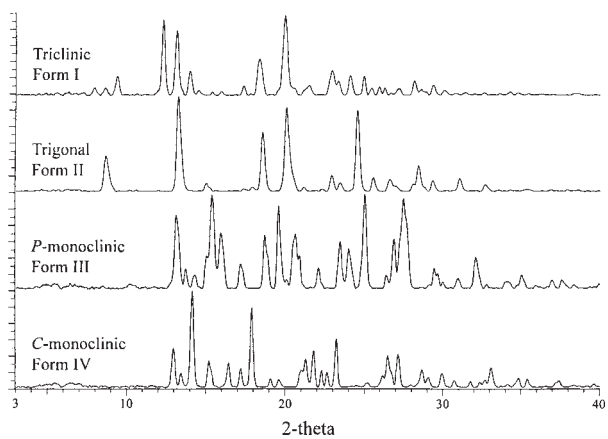

Figure 3. PXRD patterns of all four anhydrous polymorphs of CBZ.

Table 2. Powder X-ray Diffraction Peak Positions and Relative Intensities of the Four Anhydrous Polymorphs of CBZ

Triclinic (Form I)		Trigonal (Form II)		*P*-Monoclinic (Form III)		*C*-Monoclinic (Form IV)	
2θ (°)	Intensity (%)	2θ (°)	Intensity (%)	2θ (°)	Intensity (%)	2θ (°)	Intensity (%)
7.92	45	8.68	57	13.14	87	12.93	51
8.63	44	13.26	100	13.71	41	13.42	29
9.37	56	15.00	20	14.26	34	14.11	100
12.28	100	18.56	64	15.03	47	15.18	35
13.15	87	20.07	86	15.36	100	16.42	31
13.98	47	21.12	14	15.93	65	17.21	27
14.52	26	22.89	24	17.17	35	17.89	79
17.40	25	23.43	18	18.69	60	19.09	17
18.39	51	24.54	82	19.56	85	19.61	16
19.99	94	25.55	23	20.56	64	21.01	26
21.48	22	26.61	20	20.85	44	21.27	35
22.92	37	28.41	33	22.07	29	21.79	43
23.30	27	29.31	20	23.45	53	22.28	25
24.07	31	31.04	19	23.99	49	22.64	23
24.95	33	32.69	12	25.00	92	23.22	51
25.44	23			26.40	24	25.21	11
25.93	24			26.87	57	26.19	18
26.27	23			27.47	90	26.49	36
27.12	20			29.44	28	27.17	38
28.15	25			30.98	18	28.71	24
29.35	19			32.09	38	29.08	17
30.05	14			35.05	22	29.99	19
				36.98	17	30.77	12
				37.63	17	31.79	11
						32.41	11
						32.73	13
						33.11	24
						34.87	14
						35.44	13
						37.45	11

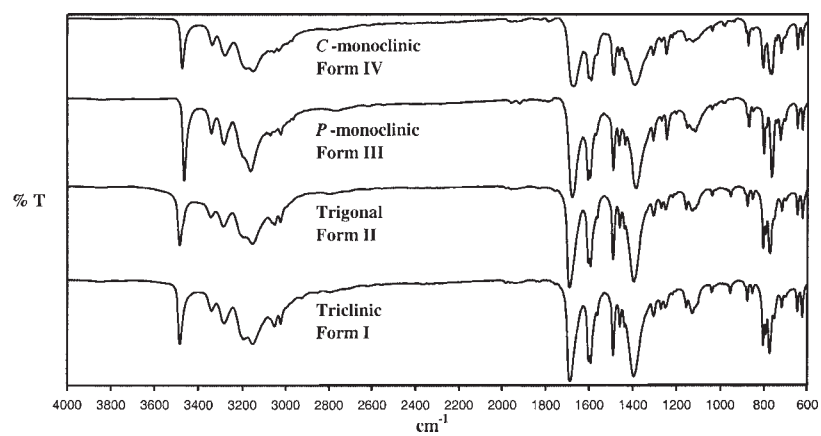

Figure 4. FTIR spectra for the four anhydrous modifications of CBZ.

Table 3. Summary of Peak Positions of the FTIR Spectra of the Four Anhydrous Modifications of CBZ

Wave Number cm^{-1}	*C*-Monoclinic (Form IV)	*P*-Monoclinic (Form III)	Trigonal (Form II)	Triclinic (Form I)
3500–3392	One sharp peak at 3474	One sharp peak at 3466	One sharp peak at 3485	One sharp peak at 3485
3392–3319	One peak at 3337	One peak at 3341	One peak at 3343	One peak at 3341
3319–3244	One peak at 3279	One peak at 3283	One peak at 3285	One peak at 3283
3244–3087	Two peaks at 3182 and 3149	One peak at 3161	One peak at 3152 with a shoulder at 3194	Two peaks at 3193 and 3151
3087–2873	Four small peaks at 3074, 3052, 3031, and 2971	Three small peaks at 3070, 3021, and 2966	Two small peaks at 3050 and 3024 with a shoulder at 3063	Three small peaks at 3051, 3023, and 2926
1731–1629	One large peak at 1674	One large peak at 1677	One large peak at 1690	One large peak at 1688
1629–1572	Double peaks at 1603 and 1591	Double peaks at 1605 and 1595	Double peaks at 1603 and 1593	Double peaks at 1602 and 1593
1534–1473	One sharp peak at 1488	One sharp peak at 1489	One sharp peak at 1489	One sharp peak at 1489
1473–1427	Double peaks at 1463 and 1437	Double peaks at 1463 and 1436	Two peaks at 1460 and 1438	Double peaks at 1460 and 1438
1427–1317	One large peak at 1394 with a shoulder at 1418	One large peak at 1386	One large peak at 1395	One large peak at 1396
1317–1190	Five peaks at 1309, 1271, 1249, 1221, and 1206	Four peaks at 1307, 1270, 1246, and 1203	Five peaks at 1305, 1270, 1251, 1218, and 1205	Five peaks at 1305, 1271, 1251, 1218, and 1206
1190–1048	Three peaks, max 1157 and 1127	Three peaks, max 1152 and 1116	Three peaks, max 1156 and 1129	Three peaks, max 1155 and 1128
1048–922	Five small peaks, max at 1039	Five small peaks, max at 1040	Five small peaks, max at 1038 and 952	Six small peaks, max at 1039 and 954
922–828	Three peaks, max at 873	Three peaks, max at 870	Three peaks, max at 876	Two peaks at 876 and 853
828–667	Seven peaks, double max at 773 and 765	Six peaks, max at 767	Six peaks, max at 803 and 772	Six peaks, max at 773
667–600	Two peaks at 647 and 625	Two peaks at 647 and 624	Two peaks at 647 and 624	Two peaks at 647 and 624

form and KBr pellets produced at 10,000 psi yielded very similar spectra indicating that a phase transformation under grinding and pressure was not taking place in any of the forms. In form I, absorptions occur at 3485, 1688, and 1396 cm^{-1}. Similarly, these peaks are at 3485, 1690, and 1395 cm^{-1} for form II and at 3466, 1677, and 1386 cm^{-1} in form III. The above values are in good agreement with those reported in the literature.[14,22,31] In form IV, the corresponding peaks are at 3474, 1674, and 1394 with a small shoulder at 1418 cm^{-1}. The spectrum of form IV also shows a double peak at 773 and 765 cm^{-1}, where only a single peak occurs at this position for the other three forms. These peaks differ by as many as 16 cm^{-1} among forms making them particularly diagnostic. However, the triclinic and trigonal spectra are nearly identical in peak positions across the entire spectrum with variations of <3 cm^{-1}. This provides additional evidence for the structural similarity of the two forms and complicates distinguishing the trigonal and triclinic forms based on IR spectra. However, IR spectroscopy has the potential to be a fast, reliable method of polymorph characterization provided that extreme care is exercised in analyzing the data.

Thermomicroscopy

The overall thermal behavior of the four CBZ polymorphs during the heating process was viewed on a hot stage under polarized light at a rate of 10°C/min. Form I showed no transformations and

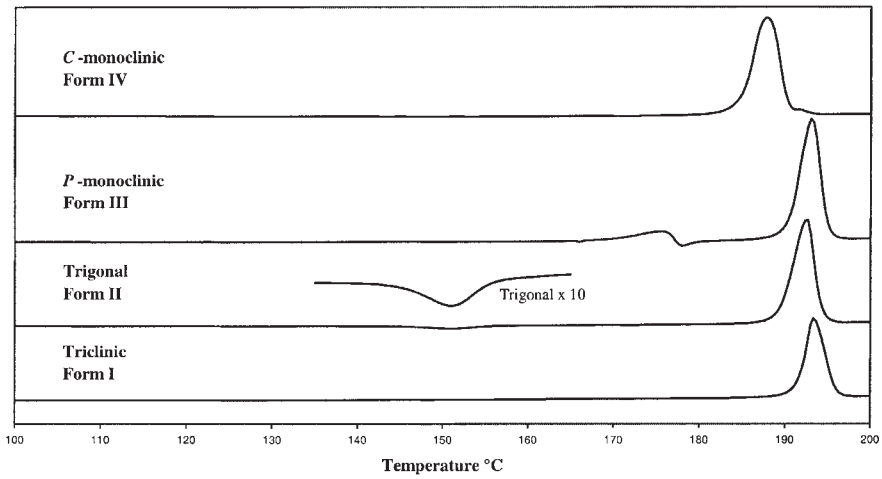

Figure 5. DSC thermograms of the four polymorphs of CBZ at a rate of 20°C/min. Inset: exothermic transformation of the trigonal to the triclinic form. Endothermic events are positive.

melted between 189 and 193°C. Form II did not melt, but instead a transformation occurred between 135 and 170°C and the new phase then melted between 188 and 192°C. The large transformation range is due, in part, to higher initiation temperatures for crystals with fewer defects as determined by observing populations of crystals during heating. Form III melts and crystallizes to a new form nearly simultaneously between 162 and 175°C. The new form subsequently melts between 189 and 193°C. Form IV showed melting and partial crystallization to a new form between 178 and 187°C, significantly higher than the transition temperatures of forms II or III. This was followed by further crystallization to produce a material that then melted between 190 and 192°C. Based on the melting point of the form that is derived from the others upon heating, it appeared that each had become form I.

The following experiments were performed to explicitly identify which form each of the three polymorphs (II–IV) had transitioned to upon heating. Form II was heated to 160°C and held at this temperature for 10 min to ensure complete conversion. Form III was heated to 182°C at 10°C/min, where complete melting and crystallization occurred during the heating process. Form IV was heated to 187°C and held at this temperature for 5 min to make certain that melting and crystallization to the new form were completed. All samples were cooled to room temperature and subjected to PXRD to identify the resulting form. This revealed that all polymorphs of CBZ transform to form I upon heating.

DSC

The thermograms for the *C*-monoclinic form IV differed significantly from those of the other three forms of CBZ (Figs. 5 and 6). DSC curves recorded at 20°C/min showed two endothermic peaks, a large peak at 187.7(1)°C followed by a small peak at 191.5(2)°C. The first endothermic peak corresponds to the melting of form IV and the second endothermic peak, similar to this phenomenon in form III, corresponds to the melting of crystallized form I. The DSC trace of form IV depends on the analytical heating rate. A decrease in scan rate results in a reduction in melting point and a more complete transformation to form I (Fig. 6). This causes a decrease in the first endotherm of melting corresponding to form IV and an increase in the second endotherm of melting corresponding to form I.

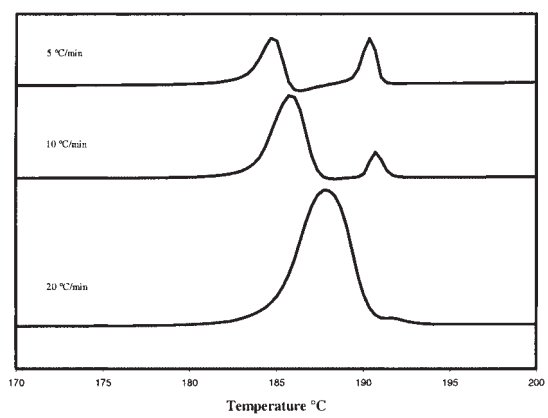

Figure 6. The DSC of form IV showing variation of melting points and melting endotherms with analytical heating rate. Endothermic events are positive.

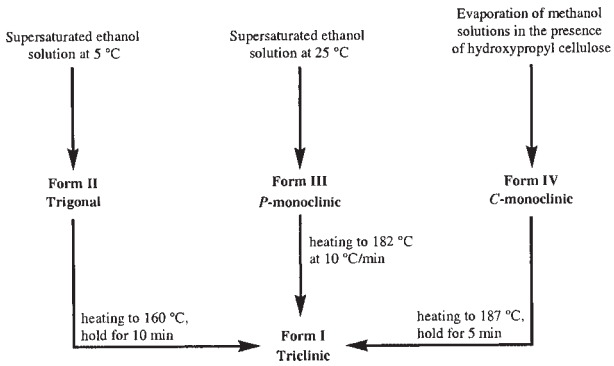

Scheme 1. Polymorphic flow chart showing the methods of preparation of the four anhydrous polymorphs of CBZ used in this study, as well as the thermal transition of forms II, III, and IV to form I.

The DSC thermogram for the *P*-monoclinic form III, recorded at 20°C/min, exhibited two endotherms and one exotherm (Fig. 5). The first endothermic peak was at 174.8(12)°C, followed immediately by an exothermic peak and subsequently a second endothermic peak at 193.2(2)°C. Thermomicroscopy showed that form III melted and subsequently crystallized to form I from 168 to 175°C, which was confirmed by the use of PXRD as mentioned above. Thus, the first endothermic peak on the DSC curve corresponds to the melting of form III, the exothermic peak shows the crystallization of form I, and the second endothermic peak coincides to the melting of form I.

The thermogram for the trigonal form II, recorded at 20°C/min, showed a small exotherm [−0.35(2) kcal/mol] in the range between 140 and 160°C and one endotherm at 192.1(5)°C (Fig. 5). The range over which the exotherm is seen on the DSC curve corresponds to the crystal transformation of form II to form I, as observed in thermomicroscopy experiments, and the endothermic peak is consistent with the melting of form I. This transformation, although overlooked by some authors perhaps because of its small enthalpy, is well entrenched in the literature.[17–19]

The DSC curve of the triclinic form I, recorded at 20°C/min, showed only one endothermic peak at 193.5(6)°C corresponding to the melting point of this form (Fig. 5). Scheme 1 summarizes the relationship of the four forms in terms of their thermal behavior and conversion to form I.

DSC revealed the following order of stability of CBZ polymorphs (Table 4): form III > form I > form IV > form II. This is the expected order based on the density rule,[40] which states: "If one modification of a molecular crystal has a lower density than the other, it may be assumed to be less stable at absolute zero." Thus, the density rule holds though only small differences in energy exist among the four forms. In fact, the energy separation is <0.7 kcal/mol between the most and least stable form, which means that for any computational method to correctly predict the proper order of stability of CBZ polymorphs, it must be accurate to much better than 1 kcal/mol, a rigorous requirement that is seldom met in practice.[41] Also notable is that the most recently characterized polymorph, form IV,[32] is more thermodynamically stable than form II, which was reported decades earlier.

CONCLUSION

With the complete structure of the triclinic polymorph of CBZ in hand, it now joins only two other compounds in the CSD that are tetramorphic.[33,34] These compounds, along with the sole examples of penta-[36] and hexamorphic[35] systems, define the current limits of structurally characterized organic solid-state isomers. Understanding the factors that give rise to these forms and their interconversion is a major challenge for experiment and theory. Currently, we are studying the thermal transformation of the trigonal form to the triclinic form of CBZ[17,18] to understand the structural changes occurring in the crystal.

Table 4. Transition Temperatures, Enthalpy of Melting, and Relative Stability of the Four Polymorphs of CBZ at a Rate of 20°C/min, and the Room Temperature Density of Each Form

	Triclinic (Form I)	Trigonal (Form II)	*P*-Monoclinic (Form III)	*C*-Monoclinic (Form IV)
Peak 1 (°C)	—	140–160	174.8(12)	187.7(1)
Peak 2 (°C)	193.5(6)	192.1(5)	193.2(2)	191.5(2)
ΔH (kcal/mol)	6.10(2)	5.72(1)	6.41(2)	5.95(3)
$\Delta(\Delta H)$ (kcal/mol)[a]	0.32(3)	0.69(2)	0	0.46(3)
Density (g/cm^3)	1.31[28]	1.24[22]	1.34[15]	1.27[32]

[a] $\Delta(\Delta H) = \Delta H_{\text{form III}} - \Delta H_{\text{other form}}$.

ACKNOWLEDGMENTS

This work was supported by start-up funds from the University of Michigan, 3M, and the NSF sponsored IGERT program for Molecularly Designed Electronic, Photonic, and Nanostructured Materials at the University of Michigan. The authors thank Jeff W. Kampf for crystal structure determination.

REFERENCES

1. Bernstein J, Davey RJ, Henck JO. 1999. Concomitant polymorphs. Angew Chem Int Ed Engl 38: 3441–3461.
2. Kariuki BM, Bauer CL, Harris KDM, Teat SJ. 2000. Polymorphism in *p*-hydroxybenzoic acid: The effect of intermolecular hydrogen bonding in controlling proton order versus disorder in the carboxylic acid dimer motif. Angew Chem Int Ed Engl 39:4485–4488.
3. Gavezzotti A, Filippini G. 1995. Polymorphic forms of organic crystals at room conditions: Thermodynamic and structural implications. J Am Chem Soc 117:12299–12305.
4. Dunitz JD, Bernstein J. 1995. Disappearing polymorphs. Acc Chem Res 28:193–200.
5. Steiner T. 1997. Unrolling the hydrogen bond properties of C–H···O interactions. Chem Commun 727–734.
6. Brittain HG. 1999. Polymorphism in pharmaceutical solids. New York: Marcel Dekker.
7. Brock CP. 1996. Investigations of the systematics of crystal packing using the Cambridge Structural Database. J Res Natl Inst Stand Technol 101:321–325.
8. Henck JO, Griesser UJ, Burger A. 1997. Polymorphism of drug substances: An economic challenge. Pharm Ind 59:165–169.
9. McCrone WC. 1957. Fusion methods in chemical microscopy. New York: Interscience Publishers.
10. Desiraju GR. 1991. The C–H···O hydrogen-bond in crystals: What is it? Acc Chem Res 24:290–296.
11. Desiraju GR. 1997. Designer crystals: Intermolecular interactions, network structures, and supramolecular synthons. Chem Commun 1475–1482.
12. Yu L, Reutzel-Edens SM, Mitchell CA. 2000. Crystallization and polymorphism of conformationally flexible molecules: Problems, patterns, and strategies. Org Process Res Dev 4:396–402.
13. Kuhnert-Brandstätter M, Kofler A, Vlachopoulos A. 1968. Beitrag zur mikroskopischen Charakterisierung und Identifizierung von Arzneimitteln unter Einbeziehung der UV-Spektrophotometrie. Sci Pharm 36:164–179.
14. Pohlmann H, Gulde C, Jahn R, Pfeifer S. 1975. Polymorphism, particle-size and blood level values of carbamazepine. Pharmazie 30:709–711.
15. Reboul JP, Cristau B, Soyfer JC, Astier JP. 1981. 5*H*-5-Dibenz[*b*,*f*]azepinecarboxamide-5 (carbamazepine). Acta Crystallogr Sect B 37:1844–1848.
16. Himes VL, Mighell AD, De Camp WH. 1981. Structure of carbamazepine: 5*H*-Dibenz[*b*,*f*]azepine-5-carboxamide. Acta Crystallogr Sect B 37: 2242–2245.
17. Kaneniwa N, Yamaguchi T, Watari N, Otsuka M. 1984. Hygroscopicity of carbamazepine crystalline powders. Yakugaku Zasshi 104:184–190.
18. Umeda T, Ohnishi N, Yokohama T, Kuroda K, Kuroda T, Tatsumi E, Matsuda Y. 1984. Kinetics of the thermal transition of carbamazepine polymorphic forms in the solid state. Yakugaku Zasshi 104:786–792.
19. Kala H, Haack U, Pollandt P, Brezesinski G. 1986. Zur Polymorphie des Carbamazepins. Acta Pharm Technol 32:72–77.
20. Lefebvre C, Guyot-Hermann AM, Draguet-Brughmans M, Bouche R, Guyot JC. 1986. Polymorphic transitions of carbamazepine during grinding and compression. Drug Dev Ind Pharm 12:1913–1927.
21. Krahn FU, Mielck JB. 1987. Relations between several polymorphic forms and the dihydrate of carbamazepine. Pharm Acta Helv 62:247–254.
22. Lowes MMJ, Caira MR, Lötter AP, van der Watt JG. 1987. Physicochemical properties and X-Ray structural studies of the trigonal polymorph of carbamazepine. J Pharm Sci 76:744–752.
23. Lisgarten JN, Palmer RA, Saldanha JW. 1989. Crystal and molecular structure of 5-carbamyl-5H-dibenzo[*b*,*f*]azepine. J Crystallogr Spectrosc Res 19: 641–649.
24. Behme RJ, Brooke D. 1991. Heat of fusion measurement of a low melting polymorph of carbamazepine that undergoes multiple-phase changes during differential scanning calorimetry analysis. J Pharm Sci 80:986–990.
25. Dugué J, Céolin R, Rouland JC, Lepage F. 1991. Polymorphism of carbamazepine: Solid-state studies on carbamazepine dihydrate. Pharm Acta Helv 66:307–310.
26. Borka L, Lonmo A, Winsnes R. 1992. Semiquantitative IR spectroscopy of the crystal polymorphs of carbamazepine: A special case in the Ph. Eur. and USP. Pharm Acta Helv 67:231–233.
27. McMahon LE, Timmins P, Williams AC, York P. 1996. Characterization of dihydrates prepared from carbamazepine polymorphs. J Pharm Sci 85:1064–1069.
28. Céolin R, Toscani S, Gardette MF, Agafonov VN, Dzyabchenko AV, Bachet B. 1997. X-ray characterization of the triclinic polymorph of carbamazepine. J Pharm Sci 86:1062–1065.

29. Roberts RJ, Payne RS, Rowe RC. 2000. Mechanical property predictions for polymorphs of sulphathiazole and carbamazepine. Eur J Pharm Sci 9:277–283.
30. Kobayashi Y, Ito S, Itai S, Yamamoto K. 2000. Physicochemical properties and bioavailability of carbamazepine polymorphs and dihydrate. Int J Pharm 193:137–146.
31. Rustichelli C, Gamberini G, Ferioli V, Gamberini MC, Ficarra R, Tommasini S. 2000. Solid-state study of polymorphic drugs: Carbamazepine. J Pharm Biomed Anal 23:41–54.
32. Lang M, Kampf JW, Matzger AJ. 2002. Form IV of carbamazepine. J Pharm Sci 91:1186–1190.
33. Nakata K, Takaki Y. 1987. Crystal structure of 2-pyrazinecarboxamide, $C_5H_5N_3O$. Memoirs of Osaka Kyoiku University, Series III 36:93–97.
34. Bar I, Bernstein J. 1985. Conformational polymorphism. IV. The crystal and molecular structures of form II, form III, and form V of 4-amino-N-2-pyridinylbenzenesulfonamide (sulfapyridine). J Pharm Sci 74:255–263.
35. Yu L, Stephenson GA, Mitchell CA, Bunnell CA, Snorek SV, Bowyer JJ, Borchardt TB, Stowell JG, Byrn SR. 2000. Thermochemistry and conformational polymorphism of a hexamorphic crystal system. J Am Chem Soc 122:585–591.
36. Hughes DS, Hursthouse MB, Threlfall T, Tavener S. 1999. A new polymorph of sulfathiazole. Acta Crystallogr Sect C 55:1831–1833.
37. Lang M, Grzesiak AL, Matzger AJ. 2002. The use of polymer heteronuclei for crystalline polymorph selection. J Am Chem Soc 124:14834–14835.
38. Bernstein J, Davis RE, Shimoni L, Chang NL. 1995. Patterns in hydrogen bonding: Functionality and graph set analysis in crystals. Angew Chem Int Ed Engl 34:1555–1573.
39. Etter MC. 1990. Encoding and decoding hydrogen-bond patterns of organic compounds. Acc Chem Res 23:120–126.
40. Burger A, Ramberger R. 1979. On the polymorphism of pharmaceuticals and other organic molecular crystals. I. Theory of thermodynamic rules. Mikrochim Acta II:259–271.
41. Lommerse JPM, Motherwell WDS, Ammon HL, Dunitz JD, Gavezzotti A, Hofmann DWM, Leusen FJJ, Mooij WTM, Price SL, Schweizer B, Schmidt MU, van Eijck BP, Verwer P, Williams DE. 2000. A test of crystal structure prediction of small organic molecules. Acta Crystallogr Sect B 56: 697–714.